THE JOURNAL OF PHYSICAL CHEMISTRY C

pubs.acs.org/JPCC Article

First-Principles Study on Methane (CH_4) Storage Properties of Graphdiyne

Wenhui Xu, Yuhong Chen,* Mingxia Song, Xiaocong Liu, Yingjie Zhao, Meiling Zhang, and Cairong Zhang

Cite This: *J. Phys. Chem. C* 2020, 124, 8110–8118 Read Online

ACCESS | Metrics & More | Article Recommendations

ABSTRACT: Graphdiyne (GDY) is a new carbon allotrope, composed of sp- and sp^2-hybridized carbon atoms, which has a larger specific surface area and a unique pore structure in comparison with graphene. Based on a first-principles analysis, the effect of Ti modification on the adsorption of methane (CH_4) by a GDY system was studied. The results indicated that modification with a Ti atom can significantly improve the CH_4 adsorption properties of GDY. The macropore position on the alkyne chain is the most stable adsorption site. A GDY system modified using a single Ti atom (Ti-GDY) can adsorb 16 CH_4 molecules on both sides, and the average adsorption energy can reach −0.225 eV/CH_4. Furthermore, a GDY system modified using two Ti atoms (2Ti-GDY) can adsorb 24 CH_4 molecules. The average adsorption energy is approximately −0.223 eV/CH_4, and the CH_4 storage capacity is 55.24 wt %. In the system, Ti and GDY are mainly connected by 2p−3d interactions between the C and Ti atoms. Hybridization between the CH_4 molecule and the substrate, in addition to the 1s H and 3d Ti orbitals, also includes electrostatic interactions. The Ti atom is in a unique macropore position along the alkyne chain, providing sufficient adsorption space and adsorption sites for CH_4. The positive electroconductivity of the CH_4 surface decreases after adsorption, reducing the influence of repulsion between the CH_4 molecules and inducing strong electrostatic interactions with the negatively charged GDY, all of which are beneficial for increasing the amount of adsorption.

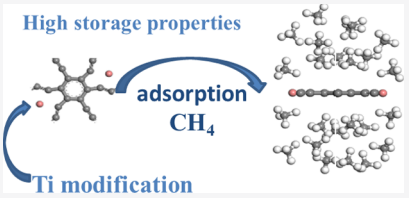

1. INTRODUCTION

The rapid socio-economic development in recent decades has been accompanied by a growing demand for energy. Traditional coal and petroleum fuels have thus been rendered insufficient to meet the energy needs of the society. Moreover, fuel combustion produces multiple pollutants such as carbon dioxide (CO_2) and carbon monoxide (CO). These gases are harmful and have serious effects on the natural environment and human health. Natural gas is a better choice owing to its abundant reserves, low price, and low levels of CO_2 emission from combustion. Natural gas is mainly composed of CH_4 (>95%), with the remaining components being a mixture of small gas molecules (including H_2S, CO, and N_2).[1] Compared to coal, CH_4 can reduce CO_2 emissions by more than 50%. Moreover, the combustion of one CH_4 produces approximately 3.1-fold the amount of heat produced by the combustion of a hydrogen (H_2). Therefore, from the viewpoint of commercial value and practical application, natural gas is more advantageous than hydrogen. Currently, natural gas is stored as liquefied natural gas[2] compressed to 200−300 bar at room temperature, compressed natural gas,[3] or adsorbed natural gas.[4,5] Owing to the high cost and high storage and transportation risks associated with the first two cases, increased attention has been paid to a variety of natural gas-adsorbing materials.

In recent years, research on CH_4 storage materials has mainly focused on molecular sieves,[6] activated carbon,[7] and metal−organic frameworks (MOFs).[8−10] Among these, MOFs show better adsorption performance and find greater application prospects, and therefore, they have received increased attention. For example, Zhao et al.[11] found that the F-modified Zr-based MOF has a storage capacity of 16.043 wt % at room temperature and high pressure, thus showing good thermal stability. Spanopouls et al.[12] reported that the weight and bulk density of the Cu-modified tbo-MOF for CH_4 storage under standard conditions can reach 26.6 wt % and 221 cm^3/cm^3, respectively. Moreover, Cu improves the storage properties of MOFs. Two-dimensional materials have also been widely explored as CH_4 storage materials owing to their light weight and high structural ordering. Moradi et al.[13] evaluated the adsorption performance of Na-modified BC_3 nanosheets on CH_4 based on the first-principles method and found that the adsorption capacity reaches 18.1 wt %. Liu et al.[14] studied the energy storage performance of a two-dimensional TiB_4 single-layer film and found that the adsorption energy of a single CH_4 was −0.41 eV and that the storage capacity reaches 10.14 wt %. Furthermore,

Received: December 30, 2019
Revised: February 27, 2020
Published: March 26, 2020

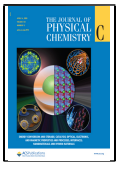

https://dx.doi.org/10.1021/acs.jpcc.9b12009
J. Phys. Chem. C 2020, 124, 8110−8118

Ghanbari et al.[15] calculated the adsorption properties of CH_4 on the surface of Ag-modified graphene and found that the adsorption energy of CH_4 is −0.166 eV, which indicates physical adsorption, thereby increasing the conductivity after adsorption. Rad et al.[16] studied the adsorption properties of NH_3 and CH_4 molecules on the surface of Pt-modified graphene. Their findings indicate that the adsorption energy of CH_4 after Pt modification increases to −0.485 eV, the charge transfer increases, and the distance between molecules is shortened. Tanaka et al.[17] studied the adsorption of CH_4 on isolated carbon nanotubes and found that the weight density reaches 19.8 wt % at room temperature. Furthermore, Chen et al.[18] found that the adsorption energy of Li-modified carbon nanotubes adsorbing CH_4 is approximately −0.464 eV, which allows for the effective separation of non-hydrocarbons in biogas. In 2012, the U.S. Department of Energy's (DOE) Advanced Research Projects Agency-Energy (ARPA-E) proposed a CH_4 storage target for vehicles. Under standard conditions, the weight and bulk density of CH_4 should be greater than 50 wt % and 350 cm^3/cm^3 (adsorbent),[19] respectively. However, most of the stored CH_4 materials are currently unable to meet these requirements.

In 2010, Li et al.[20] synthesized a two-dimensional material called graphdiyne (GDY), which is a new allotrope composed of sp and sp^2 hybrid carbon atoms. GDY has unique nanoscale pores, a two-dimensional layered conjugated framework structure, and semiconductor properties.[21−23] Consequently, it has received extensive attention both at home and abroad; moreover, it exhibits excellent characteristics for use in lithium batteries,[24−26] solar cells,[27,28] photocatalysis,[29,30] gas separation and storage,[31,32] and so forth. Lu et al.[33] studied the adsorption of Mn-modified graphyne (GY) on small gas molecules and noted that the adsorption energy of CH_4 was only −0.19 eV. Chen et al.[34] performed density functional theory calculations and found that the adsorption energy for formaldehyde molecules on Sc- and Ti-modified GDY was −2 to −2.59 eV. It was found that Sc and Ti atomic modification improved the adsorption properties of formaldehyde molecules on GDY. Zhao et al.[35] reviewed the interactions between GDY and several materials such as metal oxides and metal nanoparticles. It is believed that GDY can be used as both an electron acceptor and an electron donor, exhibiting excellent charge and electron transport properties. Moreover, GDY has a larger specific surface area and richer carbon chemical bonds compared to graphene and a unique pore structure, all of which provide more storage space and a greater number of adsorption sites for molecular adsorption. However, there are only a few studies on the adsorption properties of CH_4. Therefore, based on the density functional theory, the adsorption performance of GDY on CH_4 and the effect of Ti modification on the adsorption performance of a GDY system were considered in the present study. The adsorption energy, adsorption distance, charge transfer, charge difference density, and density of states of the system were also analyzed and discussed. It was found that Ti modification can improve the adsorption performance of CH_4 by GDY.

2. CALCULATION MODEL AND METHODS

The calculations were conducted using the CASTEP software package[36] in Materials Studio 8.0, based on the first-principles pseudopotential plane-wave method derived from the density functional theory. Furthermore, the generalized gradient approximation (GGA) in a Perdew−Burke−Ernzerhof (PBE) exchange-associative functional[37] was used along with the ultrasoft pseudopotentials to describe the interaction between electrons and ions. Because the GGA functional may underestimate the weak adsorption energy, the van der Waals correction (DFT-D)[38] method was used in calculation. As the convergence criterion for structural optimization, the force of each atom was less than 0.01 eV/Å and the self-consistent field convergence threshold was 1.0×10^{-6} eV/atom. To improve the accuracy and ensure the convergence of the calculation results, the cutoff energy of the system and the *K*-point were tested. The cutoff energy of the plane wave was set to 500 eV, and the *K*-point sampling in the Brillouin zone was set to $6 \times 6 \times 1$. This is basically consistent with the parameters of GDY described in previous research.[31,39] The calculation of the GDY unit cell satisfies the periodic boundary conditions. To reduce the interaction between layers caused by the periodic boundary conditions, the vacuum layer was selected to be 20 Å for the two-dimensional GDY structural model. For the calculation of two-Ti-modified GDY systems, the vacuum layer was too small owing to a large amount of adsorbed and layered CH_4 molecules; the vacuum layer was thus increased to 30 Å. By comparing the total energy of the system under different vacuum layers, it was evident that the size of the vacuum layer has little effect on the total adsorption energy of the system.

The binding energy (E_b) of the Ti atom on the Ti-modified GDY system was defined as follows

$$E_b = E_{Ti+GDY} - (E_{GDY} + E_{Ti}) \quad (1)$$

The average adsorption energy ($\overline{E_{ad}}$) and continuous adsorption energy (E_{ad}) of the CH_4 molecules are defined as follows

$$\overline{E_{ad}} = (E_{iCH_4+Ti+GDY} - E_{Ti+GDY} - iE_{CH_4})/i \quad (2)$$

$$E_{ad} = E_{iCH_4+Ti+GDY} - E_{(i-1)CH_4+Ti+GDY} - E_{CH_4} \quad (3)$$

where E_{GDY}, E_{Ti}, and E_{CH_4} represent the total energy of the GDY system, a free Ti atom, and a free CH_4 molecule, respectively. Here, E_{Ti+GDY} represents the total energy of the metal Ti atom-modified GDY system, whereas $E_{iCH_4+Ti+GDY}$ and $E_{(i-1)CH_4+Ti+GDY}$ indicate the total energy of i and the $(i-1)$ CH_4 molecules adsorbed into the Ti-modified GDY system, respectively.

3. RESULTS AND DISCUSSION

3.1. GDY Structure and CH_4 Adsorption Properties.

The cell structure of GDY is shown in Figure 1a. The lattice constant obtained through structural optimization was $a = b =$ 9.44 Å, which is basically consistent with the theoretically predicted lattice parameter of $a = b =$ 9.48 Å.[40] There are three

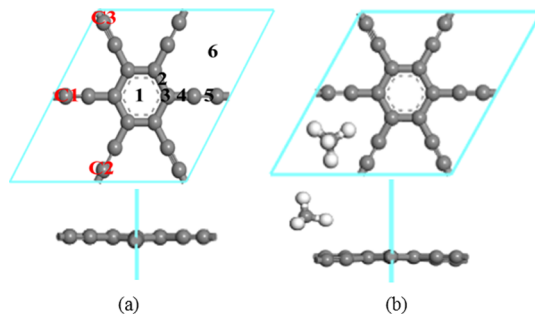

Figure 1. GDY geometry structure: (a) GDY cell; (b) GDY adsorption of CH_4 (gray and white spheres represent C and H atoms, respectively).

https://dx.doi.org/10.1021/acs.jpcc.9b12009
J. Phys. Chem. C 2020, 124, 8110−8118

types of bonds in the cell model of GDY, namely, the C−C bond on the benzene ring, the C≡C acetyl bond, and the C−C bond between the benzene ring and acetyl bond. The calculated bond lengths were 1.430, 1.232, and 1.392 Å, respectively, which agree well with the bond length measured during the experiment.[20,41] Moreover, the calculated direct band gap using the GGA/PBE functional was 0.456 eV, which coincides well with that measured within the range of 0.44−1.47 eV.[42−44] Therefore, this shows that the calculation model was well designed, and the calculation parameters were correctly set.

Different GDY systems are selected as the initial positions of the CH_4, including the central pore position of the benzene ring, the C−C bridge position on the benzene ring, the C top position on the benzene ring, the C−C bridge position where the benzene ring is connected to the acetylene bond, the bridge position on the C≡C alkyne bond, and the macropore position on the alkyne chain (shown as positions 1−6 in Figure 1a, respectively) when considering the different orientations of the CH_4 molecules (1, 2, or 3 H toward the substrate). A total of 18 adsorption structures were obtained after the structural optimization. The most stable structure for adsorption was the macropore position of the alkyne chain (as shown in Figure 1b). The three Hs in CH_4 were oriented toward the GDY, and the adsorption energy was −0.120 eV. In comparison with the storage and transportation standards of CH_4, the adsorption energy is small and a practical application is difficult to achieve.

3.2. Single-Ti-Atom-Modified GDY. *3.2.1. Adsorption Configuration of GDY Modified by a Single Ti Atom.* The modification of two-dimensional materials by alkali metals, alkaline earth metals, and transition metals can improve the adsorption properties of gas molecules. In this study, a variety of metal-modified GDYs were selected for the adsorption calculation of CH_4. The calculated binding energies of GDY modified with metal Li, Na, K, Ca, Mg, Sc, Mn, Co, Ni, Cu, and Zn were small (−0.132 to −0.558 eV), whereas the binding energies of GDY modified by the transition metals Ti, V, Fe, and Cr were larger (−0.633, −0.612, −0.724, and −0.720 eV, respectively). However, compared to the Ti-modified GDY structure, the other three structures underwent a large deformation and two-dimensional structural collapse, and the Ti atom was the lightest. Therefore, in this study, the evaluation of GDY was based on Ti atom modification. The adsorption properties of a single Ti atom at six different adsorption sites of GDY (shown as 1−6 in Figure 1a) were first investigated. By comparing the binding energy of Ti and the structural stability of the system in a Ti-modified GDY system (Ti-GDY), it was determined that the most stable adsorption site was a large pore position of the alkyne chain, which was along the plane of GDY, and the binding energy was −5.351 eV (as shown in Figure 2).

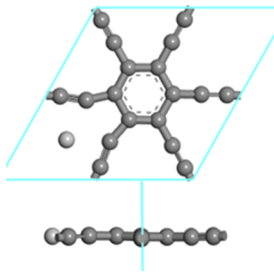

Figure 2. Most stable structures of single-Ti-modified GDY (gray and silver spheres represent C and Ti atoms, respectively).

This position is the same as the Ti modification position in the adsorption of formaldehyde molecules of Sc- and Ti-modified GDY.[34] Concurrently, the absolute value of the binding energy of Ti atoms was greater than the cohesive energy of Ti atoms (−4.85 eV);[45] the Ti atoms were thus less prone to agglomeration in the GDY model. However, the Ti atoms placed at adsorption sites 1−5 underwent large deformations in the optimized structure, and the binding energy range was −5.351 to −3.802 eV.

Based on the analysis of the Mulliken charge population (as presented in Table 1), the Ti atom in the charge of the Ti-GDY system was transferred by 1.76 e to the base GDY, which occurred owing to a strong ionic interaction. Figure 3 shows the partial wave state density (PDOS) of the Ti-GDY system. It can be seen that the valence band of the system is below the −7.481 eV energy level and is mainly composed of the s and p orbitals of C; the conduction band is within the range of −7.481−12 eV, which originates from interaction between the p orbital of the C atom and the d orbital of the Ti atom, indicating that there was a strong 2p−3d interaction between the C and Ti atoms. This is related to the Ti-modified GDY studied by Lin[46] as a catalyst for CO oxidation on the effect of Ti atoms on GDY. Because the Ti atom provides additional electrons to GDY, the conduction band of the system moves below the Fermi level, thereby transforming the GDY from a semiconductor to a metal.

3.2.2. CH_4 Adsorption Properties of Ti-GDY. The most stable structure of the CH_4 molecule adsorbed in the Ti-GDY system is shown in Figure 4a. The adsorption energy of the system was −0.633 eV, which is higher than the adsorption energy of Li-modified carbon nanotubes adsorbing CH_4[18] and Ag and Pt-modified graphene on the CH_4 molecule.[15,16] Moreover, the adsorption energy was much greater than that of the Mn-modified GY on the CH_4 molecule,[33] indicating that the modification of the Ti atom significantly improved the adsorption properties of the CH_4 molecule. Furthermore, to study the CH_4 storage of the system, CH_4 molecules were added to the system. It was found that the system could adsorb up to eight CH_4 molecules on one side (Figure 4). The analysis found that the first two CH_4 molecules were located above the Ti atom and were closer to the GDY substrate. Owing to the balance of the repulsion between the CH_4 molecules and the adsorption between the molecules and substrate, the third CH_4 molecule is adsorbed at the center of the benzene ring position and the fourth CH_4 molecule is adsorbed near the Ti atom; in addition to an increase in the number of adsorbed CH_4 molecules, owing to a limitation of the adsorption space, the CH_4 molecule gradually moves above the large hole position of the unmodified alkyne chain; the symmetry was destroyed when they adsorbed the seventh CH_4 molecule. In addition, the gas molecules were stratified when they adsorbed the eighth CH_4 molecule. When the ninth CH_4 molecule was placed on one side, the adsorption energy was positive, indicating that the gas molecules failed to adsorb on the substrate. By analyzing the Mulliken charge population (Table 1), it was found that the C atom was negatively charged, whereas the four H atoms were positively charged in the CH_4 molecule. There was a large repulsion between molecules that made it difficult for multiple CH_4 molecules to aggregate at the same adsorption site. This is consistent with the adsorption of CH_4 on the Li-modified graphene given by Xue et al.[47] who used H_2 and CH_4 mixed adsorption to reduce the repulsive forces between CH_4 molecules. However, GDY has a unique macropore position on the alkyne chain, where the modified Ti atom is on the GDY

https://dx.doi.org/10.1021/acs.jpcc.9b12009
J. Phys. Chem. C 2020, 124, 8110−8118

Table 1. Mulliken Charge Population before and after Adsorption of One CH_4 Molecule in the Ti-GDY System

	before adsorption (e)				after adsorption (e)			
atom	S	P	d	charge	s	p	d	charge
H1	0.73			0.27	0.88			0.12
H2	0.73			0.27	0.67			0.33
H3	0.73			0.27	0.75			0.25
H4	0.73			0.27	0.75			0.25
C	1.51	3.59		−1.10	1.45	3.65		−1.10
C1	1.05	3.22		−0.27	1.06	3.25		−0.31
C2	1.10	3.10		−0.20	1.11	3.11		−0.23
C3	0.95	3.14		−0.08	0.95	3.15		−0.10
Ti	2.04	5.55	2.64	1.76	1.85	5.38	2.67	2.09

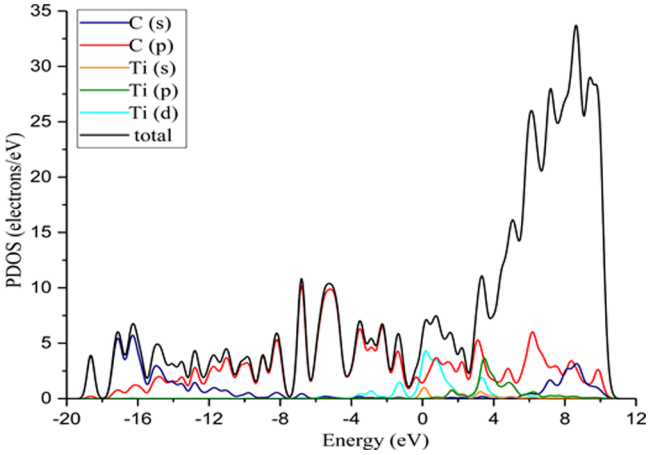

Figure 3. Partial state of the density map of the Ti-GDY system (PDOS).

plane, providing a sufficient adsorption space for CH_4. In the Ti-GDY system, the modified Ti atom was positively charged, whereas GDY was negatively charged, causing it to react strongly and interact electrostatically with the CH_4 of the negatively charged center and the positively charged surface. Therefore, the influence of the repulsion between the CH_4 molecules was reduced. The Ti-GDY system finally adsorbed eight CH_4 molecules on one side and the adsorption structure exhibited an arc shape.

Table 2 lists the average adsorption energy $\overline{E_{ad}}$ (eV), continuous adsorption energy E_{ad} (eV), distance between C atoms in CH_4 and GDY or Ti, $d_{C\text{-}GDY}$ (Å), $d_{C\text{-}Ti}$ (Å), and adsorption capacity PBW (wt %) of CH_4 in the Ti-GDY system. It was found that the adsorption energy decreases when the adsorption position of CH_4 is far from the Ti atoms and increases when the adsorption position of CH_4 is closer to the Ti atoms. This shows that Ti atoms affect its adsorption properties and play an important role in the adsorption of CH_4 molecules in the system. Moreover, the distance between the CH_4 molecule and the substrate also affects the magnitude of the adsorption energy. When the seventh CH_4 molecule, which is far from the Ti atom and is at the largest distance from GDY, is adsorbed, the continuous adsorption energy is minimal. The Ti-GDY system absorbs eight CH_4 molecules on one side, the average adsorption energy of which is −0.228 eV/CH_4, and the

Table 2. Average Adsorption Energy $\overline{E_{ad}}$ (eV), Continuous Adsorption Energy E_{ad} (eV), Distance between CH_4 and GDY or Ti, $d_{C\text{-}GDY}$ (Å), $d_{C\text{-}Ti}$ (Å), and Adsorption Capacity PBW (wt %) of CH_4 in the Ti-GDY System

number of CH_4	$\overline{E_{ad}}$ (eV)	E_{ad} (eV)	$d_{C\text{-}GDY}$ (Å)	$d_{C\text{-}Ti}$ (Å)	PBW (wt %)
1	−0.633	−0.633	2.312	2.452	5.73
2	−0.391	−0.149	3.479	4.154	10.83
3	−0.310	−0.149	3.393	5.790	15.42
4	−0.282	−0.195	3.256	4.420	19.55
5	−0.253	−0.141	2.880	9.020	23.30
6	−0.254	−0.259	3.766	7.286	26.71
7	−0.224	−0.039	4.053	7.959	29.84
8	−0.228	−0.262	3.265	5.537	32.71
16	−0.225				49.29

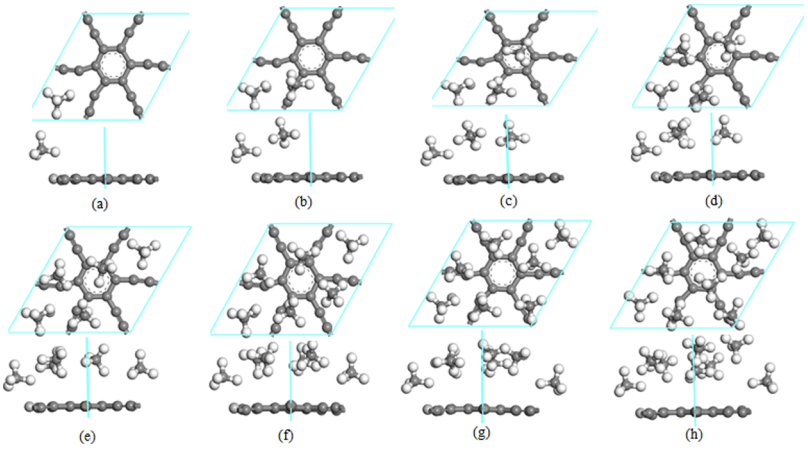

Figure 4. Geometry of CH_4 molecule adsorption by Ti-GDY: (a−h) indicate 1−8 CH_4 adsorption on one side, respectively.

https://dx.doi.org/10.1021/acs.jpcc.9b12009
J. Phys. Chem. C 2020, 124, 8110−8118

adsorption amount reaches 32.71 wt %. It can thus be calculated that Ti-GDY can adsorb 16 CH_4 molecules on its both sides (as shown in Figure 5), in which case the average adsorption energy

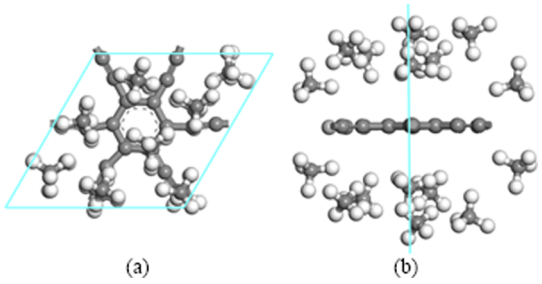

Figure 5. Geometry of single-Ti-modified GDY both-sided adsorption of CH_4 molecules: (a) top view and (b) front view.

is −0.225 eV/CH_4, and the adsorption capacity is 49.29 wt %, which is close to the requirements for DOE (50 wt %). Meanwhile, it is much larger than both the two-dimensional Na-modified BC_3 nanosheet (18.1 wt %)[13] and energy storage properties of a TiB_4 monolayer film (10.14 wt %).[14]

By analyzing the population of Mulliken before and after molecular adsorption, the charge transfer between atoms can be obtained and the interaction between the substrate and molecule during the adsorption process can be analyzed. Table 1 shows the layout of the Mulliken charge before and after the adsorption of one CH_4 molecule in the Ti-GDY system. Here, C, H1, H2, H3, and H4 represent C and H atoms in the CH_4 molecule, whereas H2 is a H atom facing upward in the CH_4 molecule (Figure 4a), which lost 0.06 electrons. The remaining H atoms in the CH_4 molecule gained electrons, whereby the nearest H1 atom from the benzene ring gained the most electrons (0.15 e), whereas the other two H atoms gained electrons (0.02 e). The charge in the C atom did not change; the CH_4 band had a weakly negative charge, whereas the positive charge on the surface decreased. Moreover, the molecules were polar, and the positive charge of H1 atoms near the substrate significantly reduced, weakening the repulsion between CH_4 molecules. Furthermore, the modified Ti atom underwent a large charge transfer (loss of electrons, 0.33 e) before and after the adsorption of CH_4 molecules. In addition, C1, C2, and C3 are the C atoms with the most charge transfer in the GDY structure (the positions of which are shown in Figure 1a), and they all gained electrons. Consequently, the electronegativity of GDY was enhanced, and the electrostatic interaction with CH_4 molecules was strengthened, creating favorable conditions for adsorption. In addition, after the adsorption of CH_4, the interaction between the Ti atom and substrate was enhanced owing to the increased charge transfer between the Ti atom and GDY. Only a limited amount of charge in the Ti-GDY system was transferred to the H atom of the CH_4 molecule, which later interacted with the H atom.

Figure 6 shows the charge differential density map of the Ti-GDY system after adsorbing one CH_4 molecule. The yellow and blue areas represent the loss and gain of the electrons, respectively. In the yellow region, the Ti atom loses electrons, whereas the H atom in the CH_4 molecule gains electrons in the blue region. Moreover, the adsorption of CH_4 molecules is mainly affected by the Ti atoms, which is consistent with the Mulliken charge population analysis shown in Table 1.

To further explore the interaction between the substrate and CH_4 molecule, the PDOS of the CH_4 molecular system

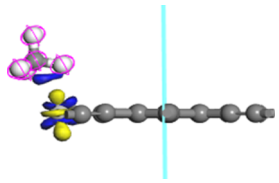

Figure 6. Charge difference density map of CH_4 molecules adsorbed by the Ti-GDY system.

adsorbed by the Ti-GDY system was analyzed. As shown in Figure 7a, the PDOS adsorbing one CH_4 molecule in the Ti-GDY system showed an increase in the DOS peak of the Ti atom compared to the pre-adsorption state, where the energy range was −8.551 to −0.942 eV. Therefore, the adsorption of the CH_4 molecule increased the interaction between the Ti atoms and substrate, which is similar to the results of the Mulliken charge population analysis. Similarly, the peak value of the total DOS valence band was improved, whereas a minor change in the DOS of the C atom occurred in the GDY, which can be attributed to the hybridization between the 3d orbit of Ti and the 1s orbit of H. Therefore, the interaction between the d orbital of Ti atoms and the s orbital of the H atom, and the p orbital of the C atoms in the first to the eighth CH_4 molecules adsorbed by Ti-GDY was further analyzed (see Figure 7b). It is evident that within the interval of −8.415−7.119 eV, the 1s orbital of H overlapped with the 3d orbital of Ti, and the broadening of the energy band for the CH_4 molecule indicates that the CH_4 molecule interacted with the Ti atom. Elsewhere, the DOS peak of the second CH_4 molecule was lower than that of the first CH_4 molecule and shifted to the right relative to the 1s orbit of the H atom of the first CH_4 molecule. This indicates that the interaction between the second CH_4 molecule and the Ti atom was slightly weaker than that of the first CH_4 molecule, which subsequently shows that the adsorption energy of the second CH_4 molecule was smaller than that of the first CH_4 molecule. Moreover, with an increase in the CH_4 molecule, the shift in the DOS peak for the CH_4 molecule was also consistent with the change in adsorption energy; when the adsorption energy reduced, the DOS peak shifted to the right, and when it increased, it shifted to the left. In the interval −6.75 to −4.57 eV, the peak of the seventh CH_4 molecule was significantly lower than that of several other CH_4 molecules, indicating that the interaction between the 1s orbital of H and the 3d orbital of Ti in the seventh CH_4 molecule was significantly weakened. Minimal adsorption energy therefore occurred, which also resulted in a delamination after the adsorption of the eighth CH_4 molecule.

3.3. Adsorption CH_4 Properties of Two-Ti-Atom-Modified GDY. To investigate the maximum CH_4 storage capacity of the system, the performance of a two-Ti-atom-modified GDY (2Ti-GDY) system for CH_4 storage was further studied. Considering the symmetry of the system and the storage space of CH_4, the Ti atoms were placed in the macropores of the acetylene chain symmetrical to the first Ti atom. The optimized structure is shown in Figure 8. Noticeably, the two Ti atoms were substantially in the same plane as the GDY substrate, but the GDY structure was slightly deformed. Furthermore, the binding energy of the second Ti atom added to the system was calculated to be approximately −6.488 eV, and the average binding energy was close to −5.913 eV. Moreover, the binding energy of the second Ti atom was larger than that of the first Ti atom, meaning that the interaction between the second Ti atom and GDY was stronger than that of the first atom.

https://dx.doi.org/10.1021/acs.jpcc.9b12009
J. Phys. Chem. C 2020, 124, 8110−8118

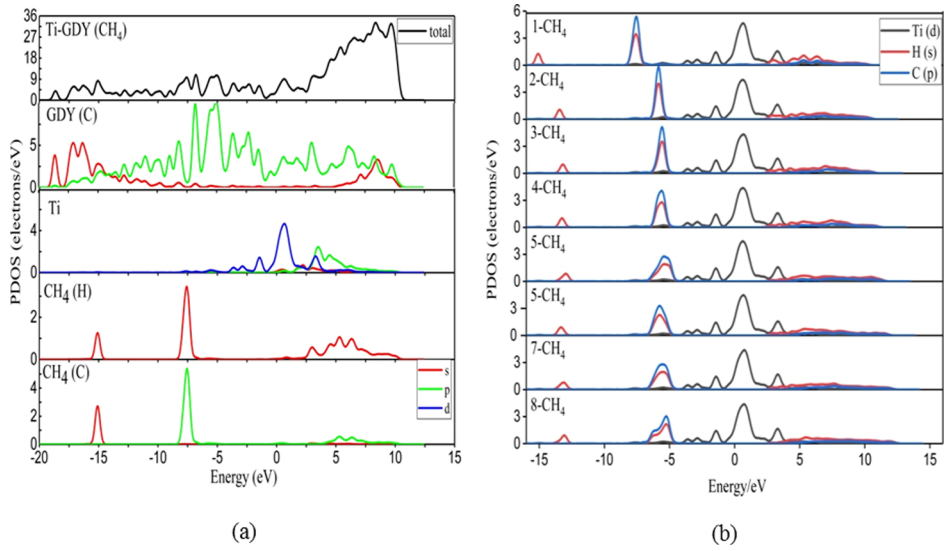

Figure 7. Density of state of adsorption of CH_4 molecules in the Ti-GDY system: (a) Ti-GDY absorbing one CH_4 molecule and (b) Ti-GDY absorbing 1−8 CH_4 molecules.

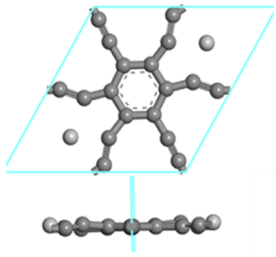

Figure 8. Most stable structures of double-Ti-modified GDY.

The 2Ti-GDY system was able to adsorb 12 CH_4 molecules on one side, the optimized geometry of which is shown in Figure 9a−l. Owing to the mutual repulsion between the CH_4 molecules and the limitation of the adsorption space, when the seventh CH_4 molecule was adsorbed, the gas molecules were stratified, that is, the first six CH_4 molecules were adsorbed into the first layer close to the Ti atoms, resembling the adsorption of a single Ti atom. However, because the addition of the second Ti atom increases the adsorption site of CH_4, the interaction between Ti atoms and CH_4 was greater than the mutual repulsion between CH_4 molecules. Thus, six CH_4 molecules were adsorbed in the second layer, and the final adsorption

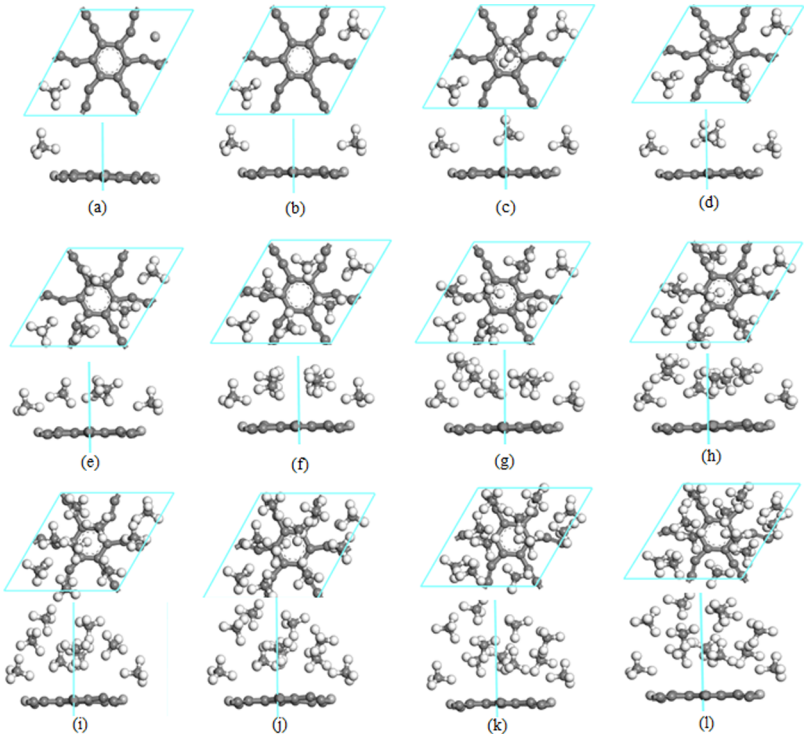

Figure 9. Geometry of 2Ti-GDY adsorbed CH_4 molecules: (a−l) indicate 1−12 CH_4 adsorption on one side, respectively.

https://dx.doi.org/10.1021/acs.jpcc.9b12009
J. Phys. Chem. C 2020, 124, 8110−8118

structure exhibited a semi-arc shape. Table 3 shows the adsorption properties calculated under these conditions.

Table 3. Average Adsorption Energy $\overline{E_{ad}}$ (eV), Continuous Adsorption Energy E_{ad} (eV), Distance between the C Atom and GDY in CH_4 $d_{C\text{-}GDY}$ (Å), and Adsorption Capacity PBW (wt %) of CH_4 in the Ti-GDY System

number of CH_4	$\overline{E_{ad}}$ (eV)	E_{ad} (eV)	PBW (wt %)	$d_{C\text{-}GDY}$ (Å)
1	−0.555	−0.555	4.89	2.250
2	−0.518	−0.481	9.33	2.459
3	−0.404	−0.175	13.37	3.271
4	−0.350	−0.188	17.06	3.509
5	−0.325	−0.228	20.46	3.236
6	−0.305	−0.203	23.58	3.849
7	−0.277	−0.110	26.47	3.124
8	−0.260	−0.142	29.15	4.227
9	−0.244	−0.118	31.64	6.028
10	−0.234	−0.140	33.96	3.442
11	−0.231	−0.202	36.13	3.250
12	−0.226	−0.168	38.16	7.164
24	−0.223		55.24	

Evidently, the second Ti atom increased the adsorption site and activity of the substrate to the CH_4 molecule, which makes up for the disadvantage of the small amount of adsorption energy of the CH_4 molecule far from the Ti atom, or the lack of absorption, when the single Ti atom was modified by GDY. The 2Ti-GDY system thus adsorbed up to 12 CH_4 molecules on one side, and the average adsorption energy was approximately −0.226 eV/CH_4, whereas the adsorption capacity reached 38.16 wt %. Notably, the adsorption energy was similar to that of a single-Ti-atom modification, but the adsorption capacity was significantly enhanced. It can thus be calculated that the 2Ti-GDY system can adsorb 24 CH_4 molecules on both sides, with the optimized geometry shown in Figure 10. The adsorption

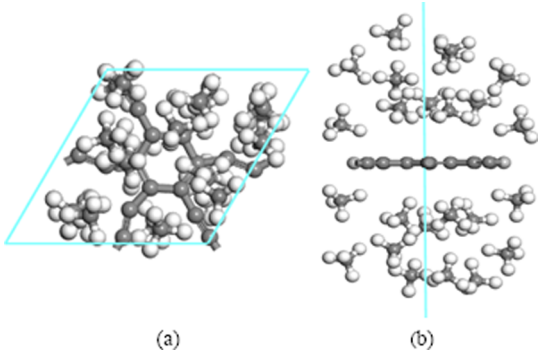

Figure 10. Geometry of 2Ti-GDY both-sided adsorption of CH_4 molecules: (a) top view and (b) front view.

structure exhibited an ellipsoidal shape with an average adsorption energy of approximately −0.223 eV/CH_4 and an adsorption capacity of 55.24 wt %. Markedly, this adsorption capacity exceeds that of the DOE standard (50 wt %), the adsorption amount of CH_4 by the MOF under metal modification (16.024−26.6 wt %),[11,12] and the CH_4 storage properties of Li-modified carbon nanotubes (19.8 wt %).[17]

A simultaneous analysis of the Mulliken charge population before and after molecular adsorption revealed that when the 2Ti-GDY system adsorbed 24 CH_4 molecules, the two Ti atoms lost electrons (0.8 and 0.79 e, respectively) and a large charge transfer occurred with the GDY. Moreover, the interaction was enhanced, and the quantity of the base GDY charge layout was −3.35 e. In addition, the negative charge was enhanced, which is favorable for the adsorption of CH_4 molecules with a positive charge on the surface. Concurrently, the CH_4 molecule closer to the Ti atom gained electrons (approximately 0.20 e) and a large charge transfer occurred between the Ti atoms, resulting in a strong interaction, which caused a large adsorption energy. However, during this process, the CH_4 molecule far from the Ti atom lost electrons (approximately 0.03 e), resulting in a CH_4 molecule with a weak positive charge, leading to minimal adsorption energy. Evidently, the adsorption of CH_4 molecules was mainly affected by Ti atoms, which is consistent with the adsorption of CH_4 molecules by the Ti-GDY system.

Figure 11 shows the changes in the average adsorption energy $\overline{E_{ad}}$ and continuous adsorption energy E_{ad} of CH_4 molecules in Ti-GDY and 2Ti-GDY systems. Based on the average adsorption energy, it is evident that the two-Ti-atom modifications significantly increased the adsorption capacity and energy. The adsorption energy of 24 CH_4 molecules in the 2Ti-GDY system and 12 CH_4 molecules in the Ti-GDY system was equivalent. Furthermore, based on the relationship of continuous adsorption energy, it is clear that the continuous adsorption energy of CH_4 in the 2Ti-GDY system was relatively stable; however, there was a significant variance in the continuous adsorption energy in the Ti-GDY system. This resulted from the reduced distance between the CH_4 molecule and the modified Ti atom owing to the two-Ti modifications, subsequently increasing the continuous adsorption energy and adsorption amount of the CH_4 molecule. Moreover, the unique pore structure of GDY provided a special modification position (in the two-dimensional plane) for the modified Ti atom. In addition, the two-dimensional structure provided sufficient adsorption space for the CH_4 molecules, and thus, the adsorption of CH_4 by the Ti-modified GDY system attained better adsorption energy and capacity.

4. CONCLUSIONS

In this study, the properties of GDY and Ti-modified GDY systems for the adsorption of CH_4 molecules were investigated based on the first-principles density functional theory. It was found that GDY weakly adsorbs CH_4 molecules. Moreover, the most stable adsorption site was the macropore position of the alkyne chain, with an adsorption energy of −0.120 eV. Moreover, Ti-atom modification can significantly improve the adsorption properties of GDY on CH_4. The most stable adsorption site was the macropore position of the alkyne chain, and the adsorption energy of a single CH_4 molecule was −0.633 eV. The Ti-GDY system was able to adsorb 16 CH_4 molecules on both sides, with the average adsorption energy reaching −0.225 eV/CH_4 and an adsorption capacity of 49.29 wt %. The 2Ti-GDY system was capable of adsorbing 24 CH_4 molecules with an average adsorption energy of approximately −0.223 eV/CH_4 and a capacity of 55.24 wt % for storing the CH_4 molecules. Moreover, it should be noted that the adsorption of CH_4 molecules by the GDY system is mainly affected by Ti atoms, and the interaction between Ti and GDY was mainly a 2p−3d interaction between C and Ti atoms. In addition to the hybridization of the 1s orbital of H and the 3d orbital of Ti, the CH_4 molecule and the substrate also included electrostatic interactions. Furthermore, GDY has a unique macropore

https://dx.doi.org/10.1021/acs.jpcc.9b12009
J. Phys. Chem. C 2020, 124, 8110−8118

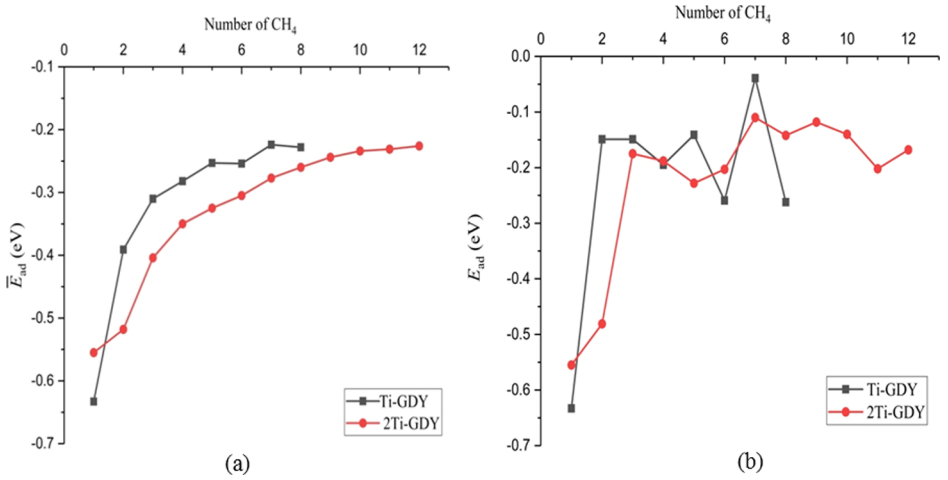

Figure 11. Changes in (a) average adsorption energy $\overline{E_{ad}}$ and (b) continuous adsorption energy E_{ad} of CH_4 molecules in Ti-GDY and 2Ti-GDY systems.

position in the alkyne chain, and thus, the modified atom Ti is on the GDY plane, which provides sufficient adsorption space and sites for CH_4. In the Ti-GDY system, the modified Ti atom was positively charged, whereas GDY was negatively charged (the negative charge of GDY was further enhanced after the adsorption of CH_4). Therefore, GDY has a strong electrostatic interaction with the CH_4 molecule possessing a negative electric center and a positively charged surface. In addition, the decrease in the positive charge on the CH_4 surface after adsorption also reduced the influence of the repulsion between CH_4 molecules, creating a favorable condition for enhancing the adsorption capacity. Therefore, we strongly believe that Ti-modified GDY will become one of the most promising materials in the storage and transport of CH_4.

AUTHOR INFORMATION

Corresponding Author

Yuhong Chen − *School of Science and State Key Laboratory of Advanced Processing and Recycling of Non-Ferrous Metals, Lanzhou University of Technology, Lanzhou 730050, China;* orcid.org/0000-0003-1597-1232; Email: chenyh@lut.cn

Authors

Wenhui Xu − *School of Science, Lanzhou University of Technology, Lanzhou 730050, China*

Mingxia Song − *School of Science, Lanzhou University of Technology, Lanzhou 730050, China*

Xiaocong Liu − *School of Science, Lanzhou University of Technology, Lanzhou 730050, China*

Yingjie Zhao − *School of Science, Lanzhou University of Technology, Lanzhou 730050, China*

Meiling Zhang − *School of Science, Lanzhou University of Technology, Lanzhou 730050, China*

Cairong Zhang − *School of Science and State Key Laboratory of Advanced Processing and Recycling of Non-Ferrous Metals, Lanzhou University of Technology, Lanzhou 730050, China;* orcid.org/0000-0002-4067-2798

Complete contact information is available at: https://pubs.acs.org/10.1021/acs.jpcc.9b12009

Author Contributions

All authors contributed to the writing of this manuscript, and all authors have given their approval to the final version.

Notes

The authors declare no competing financial interest.

ACKNOWLEDGMENTS

The authors gratefully acknowledge the financial support from the National Natural Science Foundation of China (grant no. 51562022), the Basic Scientific Research Foundation for Gansu Universities of China (grant no. 05-0342), and the Special Program for Applied Research on Super Computation of the NSFC-Guangdong Joint Fund (second phase).

REFERENCES

(1) Menon, V. C.; Komarneni, S. Porous Adsorbents for Vehicular Natural Gas Storage: a Review. *J. Porous Mater.* **1998**, *5*, 43−58.

(2) Cracknell, R. F.; Gordon, P.; Gubbins, K. E. Influence of Pore Geometry on the Design of Microporous Materials for Methane Storage. *J. Phys. Chem.* **1993**, *97*, 494−499.

(3) Burchell, T.; Rogers, M. Low Pressure Storage of Natural Gas for Vehicular Applications. *SAE Technical Paper Series*, 2000; Vol. *109*, pp 2242−2246.

(4) Peng, Y.; Krungleviciute, V.; Eryazici, I.; Hupp, J. T.; Farha, O. K.; Yildirim, T. Methane Storage in Metal-Organic Frameworks: Current Records, Surprise Findings, and Challenges. *J. Am. Chem. Soc.* **2013**, *135*, 11887−11894.

(5) Li, B.; Wen, H.-M.; Wang, H.; Wu, H.; Tyagi, M.; Yildirim, T.; Zhou, W.; Chen, B. A Porous Metal-Organic Framework with Dynamic Pyrimidine Groups Exhibiting Record High Methane Storage Working Capacity. *J. Am. Chem. Soc.* **2014**, *136*, 6207−6210.

(6) Sun, J.; Jarvi, T. D.; Conopask, L. F.; Satyapal, S.; Rood, M. J.; Rostam-Abadi, M. Direct Measurements of Volumetric Gas Storage Capacity and some New Insight Into Adsorbed Natural Gas Storage. *Energy Fuels* **2001**, *15*, 1241−1246.

(7) Policicchio, A.; Maccallini, E.; Agostino, R. G.; Ciuchi, F.; Aloise, A.; Giordano, G. Higher Methane Storage at Low Pressure and Room Temperature in new Easily Scalable Large-Scale Production Activated Carbon for Static and Vehicular Applications. *Fuel* **2013**, *104*, 813−821.

(8) Guo, Z.; Wu, H.; Srinivas, G.; Zhou, Y.; Xiang, S.; Chen, Z.; Yang, Y.; Zhou, W.; O'Keeffe, M.; Chen, B. A Metal-Organic Framework with Optimized Open Metal Sites and Pore Spaces for High Methane Storage Atroom Temperature. *Angew. Chem., Int. Ed.* **2011**, *50*, 3178−3181.

(9) Ma, S.; Zhou, H.-C. Gas Storage in Porous Metal-Organic Frameworks for Clean Energy Applications. *Chem. Commun.* **2010**, *46*, 44−53.

(10) Wu, H.; Simmons, J. M.; Liu, Y.; Brown, C. M.; Wang, X.-S.; Ma, S.; Peterson, V. K.; Southon, P. D.; Kepert, C. J.; Zhou, H.-C.; Yildirim, T.; Zhou, W. Metal-Organic Frameworks with Exceptionally High Methane Uptake: Where and How is Methane Stored? *Chem.—Eur. J.* **2010**, *16*, 5205−5214.
(11) Zhao, D.; Yu, C.; Jiang, J.; Duan, X.; Zhang, L.; Jiang, K.; Qian, G. A Fluorinated Zr-Based MOF of High Porosity for High CH_4 Storage. *J. Solid State Chem.* **2019**, *277*, 139−142.
(12) Spanopoulos, I.; Tsangarakis, C.; Klontzas, E.; Tylianakis, E.; Froudakis, G.; Adil, K.; Belmabkhout, Y.; Eddaoudi, M.; Trikalitis, P. N. Reticular Synthesis of HKUST-like tbo-MOFs with Enhanced CH_4 Storage. *J. Am. Chem. Soc.* **2016**, *138*, 1568−1574.
(13) Moradi, M.; Peyghan, A. A. Role of Sodium Decoration on the Methane Storage Properties of BC_3 Nanosheet. *Struct. Chem.* **2014**, *25*, 1083−1090.
(14) Liu, Z.; Wu, E.; Li, J.; Liu, S. Energy Storage Properties of a Two-Dimensional TiB_4 Monolayer. *Phys. Chem. Chem. Phys.* **2019**, *21*, 13151−13156.
(15) Ghanbari, R.; Safaiee, R.; Golshan, M. M. A Dispersion-Corrected DFT Investigation of CH_4 Adsorption by Silver-Decorated Monolayer Graphene in the Presence of Ambient Oxygen Molecules. *Appl. Surf. Sci.* **2018**, *457*, 303−314.
(16) Rad, A. S.; Pazoki, H.; Mohseni, S.; Zareyee, D.; Peyravi, M. Surface Study of Platinum Decorated Graphene Towards Adsorption of NH_3 and CH_4. *Mater. Chem. Phys.* **2016**, *182*, 32−38.
(17) Tanaka, H.; El-Merraoui, M.; Steele, W. A.; Kaneko, K. Methane Adsorption on Single-Walled Carbon Nanotube: a Density Functional Theory Model. *Chem. Phys. Lett.* **2002**, *352*, 334−341.
(18) Chen, J.-J.; Li, W.-W.; Li, X.-L.; Yu, H.-Q. Improving Biogas Separation and Methane Storage with Multilayer Graphene Nanostructure Via Layer Spacing Optimization and Lithium Doping: a Molecular Simulation Investigation. *Environ. Sci. Technol.* **2012**, *46*, 10341−10348.
(19) The U.S. Department of Energy's Advanced Research Projects Agency-Energy DE-FOA-0000672: Methane Opportunities for Vehicular Energy (MOVE). DOE Available from: https://arpa-e-foa.energy.gov/Default.aspx?Search=move&SearchType=. 2012.
(20) Li, G.; Li, Y.; Liu, H.; Guo, Y.; Li, Y.; Zhu, D. Architecture of Graphdiyne Nanoscale Films. *Chem. Commun.* **2010**, *46*, 3256−3258.
(21) Li, Y.; Xu, L.; Liu, H.; Li, Y. Graphdiyne and Graphyne: from Theoretical Predictions to Practical Construction. *Chem. Soc. Rev.* **2014**, *43*, 2572−2586.
(22) Kang, J.; Wei, Z.; Li, J. Graphyne and Its Family: Recent Theoretical Advances. *ACS Appl. Mater. Interfaces* **2019**, *11*, 2692−2706.
(23) Gao, X.; Liu, H.; Wang, D.; Zhang, J. Graphdiyne: Synthesis, Properties, and Applications. *Chem. Soc. Rev.* **2019**, *48*, 908−936.
(24) Makaremi, M.; Mortazavi, B.; Rabczuk, T.; Ozin, G. A.; Singh, C. V. Theoretical Investigation: 2D N-Graphdiyne Nanosheets as Promising Anode Materials for Li/Na Rechargeable Storage Devices. *ACS Appl. Nano Mater.* **2018**, *2*, 127−135.
(25) Huang, C.; Zhang, S.; Liu, H.; Li, Y.; Cui, G.; Li, Y. Graphdiyne for High Capacity and Long-Life lithium Storage. *Nano Energy* **2015**, *11*, 481−489.
(26) Zhang, S.; Liu, H.; Huang, C.; Cui, G.; Li, Y. Bulk Graphdiyne Powder Applied for Highly Efficient Lithium Storage. *Chem. Commun.* **2015**, *51*, 1834−1837.
(27) Kuang, C.; Tang, G.; Jiu, T.; Yang, H.; Liu, H.; Li, B.; Luo, W.; Li, X.; Zhang, W.; Lu, F.; Fang, J.; Li, Y. Highly Efficient Electron Transport Obtained by Doping PCBM with Graphdiyne in Planar-Heterojunction Perovskite Solar Cells. *Nano Lett.* **2015**, *15*, 2756−2762.
(28) Xiao, J.; Shi, J.; Liu, H.; Xu, Y.; Lv, S.; Luo, Y.; Li, D.; Meng, Q.; Li, Y. Efficient $CH_3NH_3PbI_3$ Perovskite Solar Cells Based on Graphdiyne (GD)-Modified P3HT Hole-Transporting Material. *Adv. Energy Mater.* **2015**, *5*, 1401943.
(29) Wang, S.; Yi, L.; Halpert, J. E.; Lai, X.; Liu, Y.; Cao, H.; Yu, R.; Wang, D.; Li, Y. A Novel and Highly Efficient Photocatalyst Based on P25-Graphdiyne Nanocomposite. *Small* **2012**, *8*, 265−271.
(30) Yang, N.; Liu, Y.; Wen, H.; Tang, Z.; Zhao, H.; Li, Y.; Wang, D. Photocatalytic Properties of Graphdiyne and Graphene Modified TiO_2: from Theory to Experiment. *ACS Nano* **2013**, *7*, 1504−1512.
(31) Qiu, H.; Xue, M.; Shen, C.; Zhang, Z.; Guo, W. Graphynes for Water Desalination and Gas Separation. *Adv. Mater.* **2019**, *31*, 1803772.
(32) Meng, Z.; Zhang, X.; Zhang, Y.; Gao, H.; Wang, Y.; Shi, Q.; Rao, D.; Liu, Y.; Deng, K.; Lu, R. Graphdiyne as a High-Efficiency Membrane for Separating Oxygen from Harmful Gases: A First-Principles Study. *ACS Appl. Mater. Interfaces* **2016**, *8*, 28166−28170.
(33) Lu, Z.; Lv, P.; Ma, D.; Yang, X.; Li, S.; Yang, Z. Detection of Gas Molecules on Single Mn Adatom Adsorbed Graphyne: a DFT-D Study. *J. Phys. D: Appl. Phys.* **2018**, *51*, 065109.
(34) Chen, X.; Gao, P.; Guo, L.; Wen, Y.; Fang, D.; Gong, B.; Zhang, Y.; Zhang, S. High-Efficient Physical Adsorption and Detection of Formaldehyde using Sc- and Ti-Decorated Graphdiyne. *Phys. Lett. A* **2017**, *381*, 879−885.
(35) Yasong, Z.; Lijuan, Z.; Jian, Q.; Quan, J.; Kaifeng, L.; Dan, W. Graphdiyne with Enhanced Ability for Electron Transfer. *Acta Phys. Sin.* **2018**, *34*, 1048−1060.
(36) Segall, M. D.; Lindan, P. J. D.; Probert, M. J.; Pickard, C. J.; Hasnip, P. J.; Clark, S. J.; Payne, M. C. First-Principles Simulation: Ideas, Illustrations and the CASTEP Code. *J. Phys.: Condens. Matter* **2002**, *14*, 2717.
(37) Perdew, J. P.; Burke, K.; Ernzerhof, M. Generalized Gradient Approximation Made Simple. *Phys. Rev. Lett.* **1996**, *77*, 3865.
(38) Björkman, T.; Gulans, A.; Krasheninnikov, A. V.; Nieminen, R. M. Van der Waals Bonding in Layered Compounds from Advanced Density-Functional First-Principles Calculations. *Phys. Rev. Lett.* **2012**, *108*, 235502.
(39) Ebadi, M.; Reisi-Vanani, A.; Houshmand, F.; Amani, P. Calcium-Decorated Graphdiyne as a High Hydrogen Storage Medium: Evaluation of the Structural and Electronic Properties. *Int. J. Hydrogen Energy* **2018**, *43*, 23346−23356.
(40) Long, M.; Tang, L.; Wang, D.; Li, Y.; Shuai, Z. Electronic Structure and Carrier Mobility in Graphdiyne Sheet and Nanoribbons: Theoretical Predictions. *ACS Nano* **2011**, *5*, 2593−2600.
(41) Baughman, R. H.; Eckhardt, H.; Kertesz, M. Structure-Property Predictions for new Planar Forms of Carbon: Layered Phases Containing sp^2 and sp Atoms. *J. Chem. Phys.* **1987**, *87*, 6687−6699.
(42) Bu, H.; Zhao, M.; Wang, A.; Wang, X. First-Principles Prediction of the Transition from Graphdiyne to a Superlattice of Carbon Nanotubes and Graphene Nanoribbons. *Carbon* **2013**, *65*, 341−348.
(43) Srinivasu, K.; Ghosh, S. K. Graphyne and Graphdiyne: Promising Materials for Nanoelectronics and Energy Storage Applications. *J. Phys. Chem. C* **2012**, *116*, 5951−5956.
(44) Luo, G.; Qian, X.; Liu, H.; Qin, R.; Zhou, J.; Li, L.; Gao, Z.; Wang, E.; Mei, W.-N.; Lu, J. Quasiparticle Energies and Excitonic Effects of the Two-Dimensional Carbon Allotrope Graphdiyne: Theory and Experiment. *Phys. Rev. B: Condens. Matter Mater. Phys.* **2011**, *84*, 075439.
(45) Chen, M.; Yang, X.-B.; Cui, J.; Tang, J.-J.; Gan, L.-Y.; Zhu, M.; Zhao, Y.-J. Stability of Transition Metals on Mg (0001) Surfaces and Their Effects on Hydrogen Adsorption. *Int. J. Hydrogen Energy* **2012**, *37*, 309−317.
(46) Lin, Z.-Z. Graphdiyne-Supported Single-Atom Sc and Ti Catalysts for High-Efficient CO Oxidation. *Carbon* **2016**, *108*, 343−350.
(47) Xue, Q.; Wu, M.; Zeng, X. C.; Jena, P. Co-mixing Hydrogen and Methane may Double the Energy Storage Capacity. *J. Mater. Chem. A* **2018**, *6*, 8916−8922.

https://dx.doi.org/10.1021/acs.jpcc.9b12009
J. Phys. Chem. C 2020, 124, 8110−8118